View Article Online
View Journal

MedChemComm

Accepted Manuscript

This article can be cited before page numbers have been issued, to do this please use: Y. Tian, J. Jin, X. Wang, W. Han, G. Li, W. Zhou, Q. Xiao, J. Qi, X. Chen and D. Yin, *Med. Chem. Commun.*, 2013, DOI: 10.1039/C3MD00079F.

This is an *Accepted Manuscript*, which has been through the RSC Publishing peer review process and has been accepted for publication.

Accepted Manuscripts are published online shortly after acceptance, which is prior to technical editing, formatting and proof reading. This free service from RSC Publishing allows authors to make their results available to the community, in citable form, before publication of the edited article. This *Accepted Manuscript* will be replaced by the edited and formatted *Advance Article* as soon as this is available.

To cite this manuscript please use its permanent Digital Object Identifier (DOI®), which is identical for all formats of publication.

More information about *Accepted Manuscripts* can be found in the **Information for Authors**.

Please note that technical editing may introduce minor changes to the text and/or graphics contained in the manuscript submitted by the author(s) which may alter content, and that the standard **Terms & Conditions** and the **ethical guidelines** that apply to the journal are still applicable. In no event shall the RSC be held responsible for any errors or omissions in these *Accepted Manuscript* manuscripts or any consequences arising from the use of any information contained in them.

View Article Online
DOI: 10.1039/C3MD00079F

Design, synthesis and docking-based 3D-QSAR study of novel 2-substituted 2-aminopropane-1, 3-diols as potent and selective agonists of sphingosine-1-phosphate 1 ($S1P_1$) receptor

Yulin Tian[a], Jing Jin[a], Xiaojian Wang[b], Weijuan Han[b], Gang Li[b], Wanqi Zhou[a], Qiong Xiao[a], Jianguo Qi[a], Xiaoguang Chen[a], Dali Yin[a,*]

A series of 2-substituted 2-aminopropane-1, 3-diols were designed and synthesized as selective $S1P_1$ agonists. COMFA and COMSIA models were established based on molecular docking alignment, which will be helpful in the design of novel, potent and selective $S1P_1$ agonists.

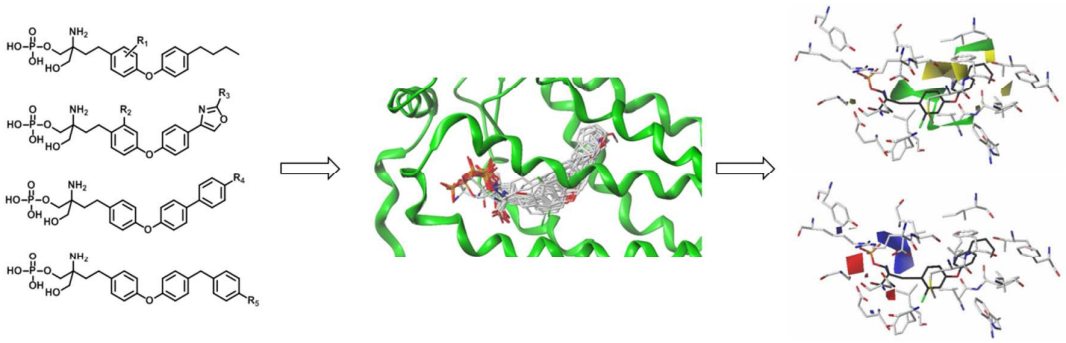

Published on 03 July 2013. Downloaded on 18/07/2013 09:13:58.

Medicinal Chemistry Communications Accepted Manuscript

View Article Online
DOI: 10.1039/C3MD00079F

Design, synthesis and docking-based 3D-QSAR study of novel 2-substituted 2-aminopropane-1, 3-diols as potent and selective agonists of sphingosine-1-phosphate 1 ($S1P_1$) receptor

Yulin Tian[a], Jing Jin[a], Xiaojian Wang[b], Weijuan Han[b], Gang Li[b], Wanqi Zhou[a], Qiong Xiao[a], Jianguo Qi[a], Xiaoguang Chen[a], Dali Yin[a,*]

[a] State Key Laboratory of Bioactive Substances and Functions of Natural Medicines, Institute of Materia Medica, Peking Union Medical College and Chinese Academy of Medical Sciences, Beijing 100050, PR China

[b] Department of Medicinal Chemistry, Beijing Key Laboratory of Active Substances Discovery and Drugability Evaluation, Institute of Materia Medica, Peking Union Medical College and Chinese Academy of Medical Sciences, Beijing 100050, PR China

Published on 03 July 2013. Downloaded on 18/07/2013 09:13:58.

Abstract

Spingosine-1-phosphate receptor 1 ($S1P_1$) has been actively pursued as an important therapeutic target in immune regulation. A series of 2-substituted 2-aminopropane-1, 3-diols were designed and synthesized as selective $S1P_1$ agonists. Most of the compounds with a biphenyl ether scaffold showed moderate to excellent $S1P_1/S1P_3$ selectivity. Compound **40c** is identified as a potent $S1P_1$ agonist with 350-fold $S1P_1/S1P_3$ selectivity. **39c**, the alcohol form of **40c** exerted good lymphopenia activity *in vivo* but with weak influence on heart rate. To investigate the SARs of 2-substituted 2-aminopropane-1, 3-diols in more details, COMFA (q^2=0.547, r^2=0.986) and COMSIA (q^2=0.544, r^2=0.943) models were established based on molecular docking alignment, which were validated with high reliability in predicting activities of agonists. The 3D-QSAR models will be helpful in the design of novel, potent and selective $S1P_1$ agonists.

Key words

2-substituted 2-aminopropane-1, 3-diols, $S1P_1$ agonists, selectivity, docking, 3D-QSAR

* Corresponding author. Tel.: + 86 10 63165248; fax: + 86 10 63165248.

E-mail address: yindali@imm.ac.cn

Medicinal Chemistry Communications Accepted Manuscript

View Article Online
DOI: 10.1039/C3MD00079F

Published on 03 July 2013. Downloaded on 18/07/2013 09:13:58.

Introduction

Sphingosine-1-phosphate (**1**, S1P) is an endogenous lysophoshpolipid that could modulate multiple downtream signaling pathways by interacting with five receptor subtypes (sphingosine-1-phosphate receptor subtype 1-5, $S1P_{1-5}$). It could regulate a variety of cellular functions, including differentiation, survival, proliferation and chemotaxis.[1] *In vivo*, S1P affects many important physiological processes, such as angiogenesis, endothelial barrier enhancement, airway and blood vessel constriction, heart rate modulation and bone homeostasis.[2]

Recently, spingosine-1-phosphate receptor 1 ($S1P_1$) has been actively pursued as an important therapeutic target due to its essential role played in immune regulation.[3] One of the $S1P_1$ modulators, FTY720 (**2**), is approved for treating multiple sclerosis in 2010.[4] Besides $S1P_1$, FTY720 is also found to be an agonist to three other S1P receptors ($S1P_{3,\ 4,\ 5}$) after being phosphorylated to its monophosphate ester (**3**, FTY720-P) *in vivo* by sphingosine kinase 2 (SPHK2).[5] Interacting with $S1P_1$ receptor by FTY720-P (**3**) results in lymphopenia through sequestering lymphocytes in secondary lymphoid organs.[6] However, a number of side effects of FTY720 such as bradycardia and hypertension were discovered in preclinical development and clinical trials.[7] KRP203(**4**), an analog of FTY720, is phosphorylated *in vivo* to KRP203-P (**5**), which is a more selective agonist of $S1P_1$ receptor and is believed to be safer than FTY720,[8] therefore has great potential in the treatment of autoimmune diseases and in the prevention of transplant rejection.

Our group has sought to discover new potent $S1P_1$ agonists with low potency on $S1P_3$ in order to retain the positive therapeutic properties and attenuate the potential risk of adverse effects. Based on literature precedent, the polar head group of FTY720-P is a key part forming salt bridge with amino acid residues in $S1P_1$ receptor.[9] Therefore, a series of new $S1P_1$ agonists keeping the polar head group with different lipophilic tail has been designed and synthesized (Scheme **1-4**). We first inserted phenyl rings into different positions along the aliphatic chain of FTY720 and obtained compounds **14a-i**, among which **14i** with a biphenyl ether scaffold showed moderate $S1P_1/S1P_3$ selectivity. This led to the design and synthesis of a series of compounds bearing this biphenyl ether scaffold (**21a-e**, **25a-c**, **30a-c** and **33**), as well as compounds with substituents on one of the phenyl ring (**40a-c** and **47).** Meanwhile, we also investigated compounds with more rigid biphenyl scaffold (**54a-b**).

To investigate SARs of 2-substituted 2-aminopropane-1, 3-diols in more details, all these compounds synthesized were docked into the binding site of $S1P_1$ receptor based on a crystal structure reported recently.[10] A docking-based 3D-QSAR model was successfully constructed using approaches of comparative molecular field analysis (COMFA)[11] and comparative molecular similarity indices analysis (COMSIA)[12]. The 3D-QSAR models will be helpful in the design of novel, potent and selective $S1P_1$ agonists.

Medicinal Chemistry Communications Accepted Manuscript

View Article Online
DOI: 10.1039/C3MD00079F

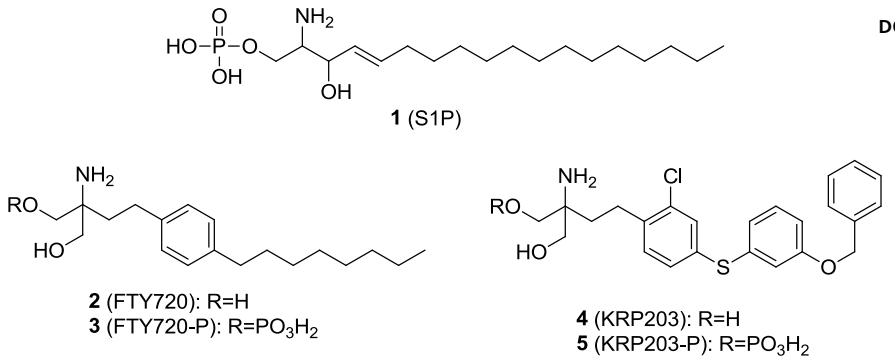

Figure 1 Structures of S1P, FTY720, FTY720-P, KRP203 and KRP203-P.

Results and discussions

Chemistry

The syntheses of compounds **14a-i** were described in Scheme **1**. Friedel-Crafts acylation of the aromatic ring with chloroacetyl chloride afforded **7a-i**. Subsequent replacement of chloro with diethyl acetamidomalonate gave **8a-i**. **9a-i** were obtained by triethylsilane / titanium tetrachloride reduction of the carbonyl.[13] Reduction of **9a-i** in the presence of $NaBH_4/K_2HPO_4$ buffer gave diols **10a-i**. Hydrolysis of amide **10a-i** with NaOH afforded compounds **11a-i**. Then the primary amino was protected with CbzCl to give compounds **12a-i**. One of hydroxyl groups was phosphorylated by tetrabenzyl pyrophosphate with silver(I) oxide and tetra-*n*-hexylammonium iodide to give compounds **13a-i**. Desired phosphate **14a-i** were obtained by removing all protective groups through hydrogenolysis.[14]

Scheme **2** illustrates the syntheses of compounds **21a-e**, **25a-c**, **30a-c** and **33**. **17** was prepared after Friedel-Crafts acylation of **15** and condensation with diethyl acetamidomalonate. Acylation of **17** with benzoyl chloride gave **18a-e**. The benzyl carbonyl groups of **18a-e** were reduced to methylene followed by removal of protecting groups and phosphorylation to afford compounds **21a-e**. **22** was achieved by carbonyl reduction of **17**. Compounds **25a-c** were synthesized from **22** through Suzuki coupling, followed by removal of protecting groups and phosphorylation. Acylation of **22** with chloroacetyl chloride afforded **26**. Replacement of chloro with carboxylic acid gave esters **27a-c**. The ring closing of **27a-c** with acetamide gave **28a-c** or **31**. Finally compounds **30a-c** and **33** were obtained by removing protecting groups and phosphorylation.

Compounds **40a-c** and **47** were prepared as outlined in Scheme **3**. Acylation of **34** with *n*-butyryl chloride or chloroacetyl chloride afforded **35** or **41**, respectively. **42** was achieved after esterification and ring closure. Substituted phenols were coupling with **35** or **42** to afford phenyl ether **36a-c** or **43**. Acylation, condensation, carbonyl reduction, removal of protecting groups and phosphorylation were proceeding successively to give compounds **40a-c** and **47**.

The syntheses of compounds **54a-b** were carried out with similar procedures to those of compounds **30a-c**, as shown in Scheme **4**.

Published on 03 July 2013. Downloaded on 18/07/2013 09:13:58.

Medicinal Chemistry Communications Accepted Manuscript

View Article Online
DOI: 10.1039/C3MD00079F

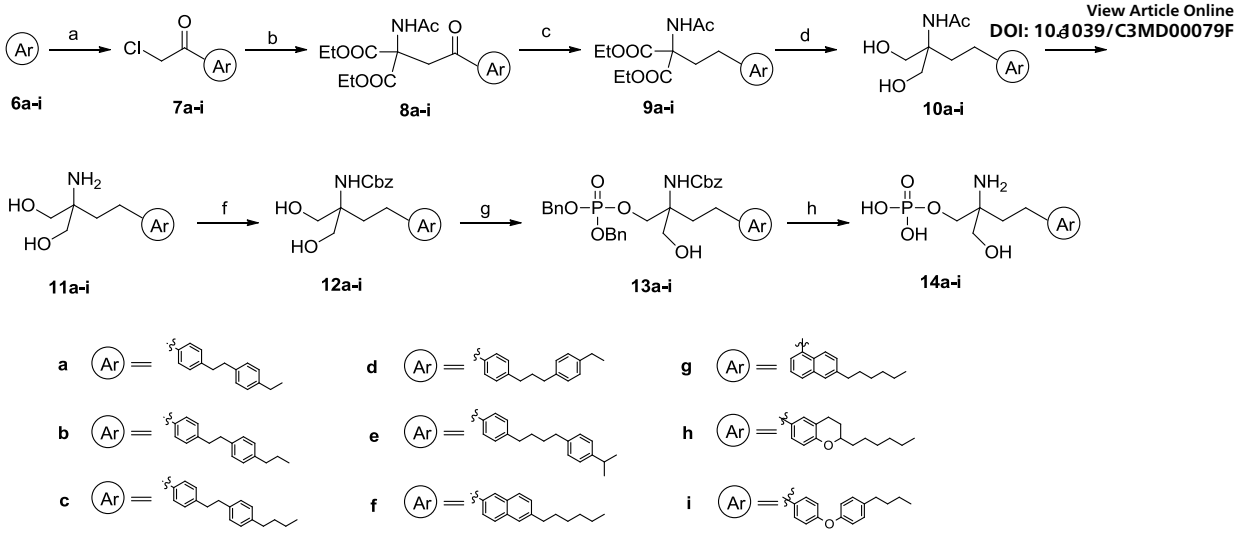

Scheme 1. Reagents and conditions: (a)chloroacetylchloride, $AlCl_3$, CH_2Cl_2, 0°C to r.t., 2h; (b) diethyl acetamidomalonate, NaH, THF, 70°C, 12h; (c) Et_3SiH, $TiCl_4$, CH_2Cl_2, r.t., 12h; (d) $NaBH_4$, K_2HPO_4 buffer, EtOH, rt, 12h; (e)NaOH, MeOH, 80°C, 8h; (f)CbzCl, $NaHCO_3$, ethyl acetate, rt, 4h; (g)TBPP, Ag_2O, Hex_4NI, CH_2Cl_2, rt, 20h; (h) H_2, Pd/C, MeOH, rt, 8h.

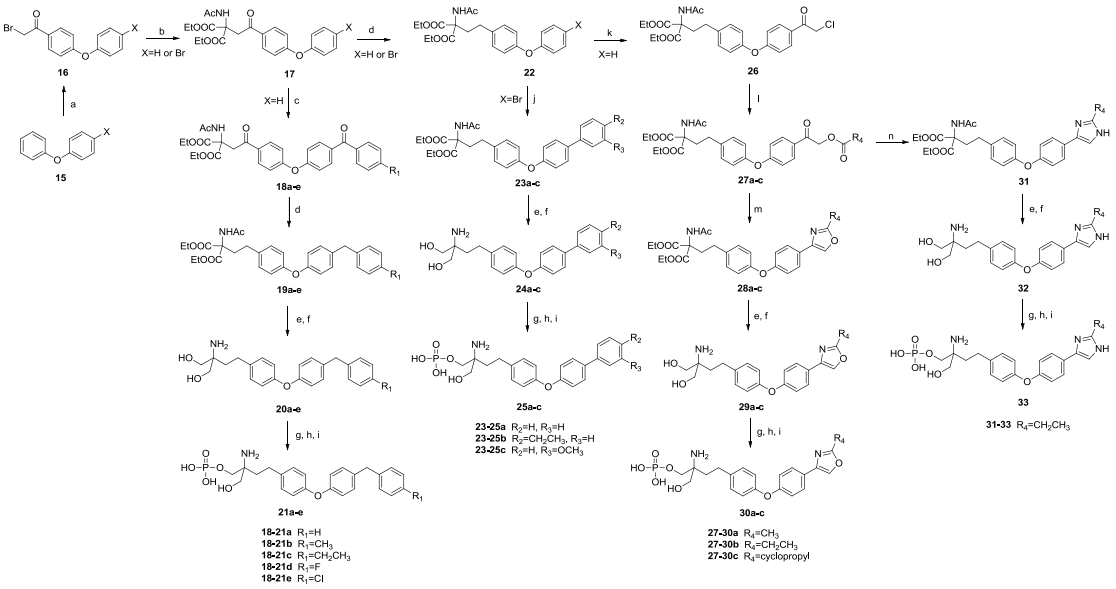

Scheme 2. Reagents and conditions: (a) bromoacetyl bromide, $AlCl_3$, CH_2Cl_2, 0°C to r.t., 2h; (b) diethyl acetamidomalonate, NaH, THF, 70°C, 12h; (c)benzoyl chloride, $AlCl_3$, CH_2Cl_2, 0°C to r.t., 4h. (d) Et_3SiH, $TiCl_4$, CH_2Cl_2, r.t., 12h; (e) $NaBH_4$, K_2HPO_4 buffer, EtOH, rt, 12h; (f)NaOH, MeOH, 80°C, 8h; (g)CbzCl, $NaHCO_3$, ethyl acetate, rt, 4h; (h)TBPP, Ag_2O, Hex_4NI, CH_2Cl_2, rt, 20h; (i) H_2, Pd/C, MeOH, rt, 8h; (j) phenylboronic acid, $Pd(PPh)_4$, 2M Na_2CO_3, toluene/EtOH, reflux, 3h; (k)chloroacetylchloride, $AlCl_3$, CH_2Cl_2, 0°C to r.t., 5h; (l) carboxylic acid, Et_3N, CH_3CN, reflux, 2h; (m) acetamide, BF_3 Et_2O, xylene, reflux, 40h; (n) acetamide, xylene, reflux, 40h;

Published on 03 July 2013. Downloaded on 18/07/2013 09:13:58.

Medicinal Chemistry Communications Accepted Manuscript

View Article Online
DOI: 10.1039/C3MD00079F

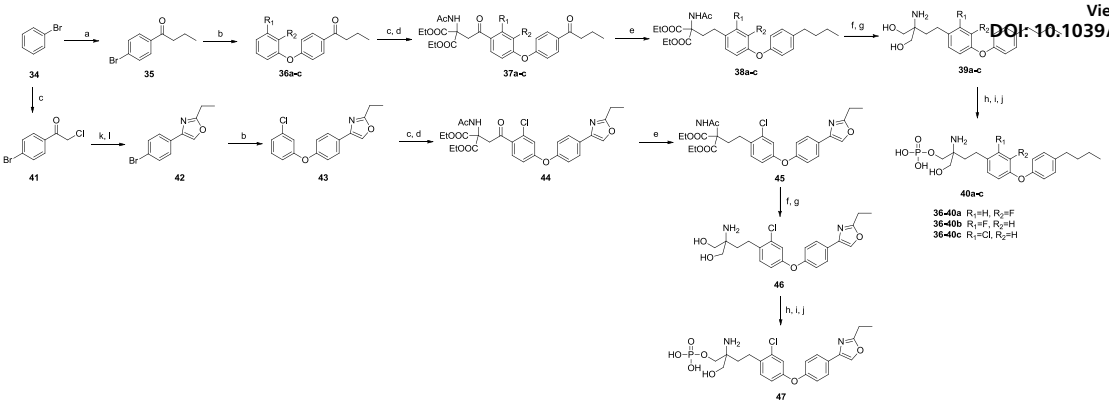

Scheme 3. Reagents and conditions: (a) *n*-butyryl chloride, $AlCl_3$, CH_2Cl_2, 0°C to r.t., 2h; (b)phenol, Cs_2CO_3, CuBr, DMF, 150°C, 20h; (c) chloroacetylchloride, $AlCl_3$, CH_2Cl_2, 0°C to r.t., 2h. (d) diethyl acetamidomalonate, NaH, THF, 70°C, 12h; (e) Et_3SiH, $TiCl_4$, CH_2Cl_2, r.t., 12h; (f) $NaBH_4$, K_2HPO_4 buffer, EtOH, rt, 12h; (g) NaOH, MeOH, 80°C, 8h; (h)CbzCl, $NaHCO_3$, ethyl acetate, rt, 4h; (i)TBPP, Ag_2O, Hex_4NI, CH_2Cl_2, rt, 20h; (j) H_2, Pd/C, MeOH, rt, 8h; (k) propanoic acid, Et_3N, CH_3CN, reflux, 2h; (l) acetamide, $BF_3 \cdot Et_2O$, xylene, reflux, 40h;

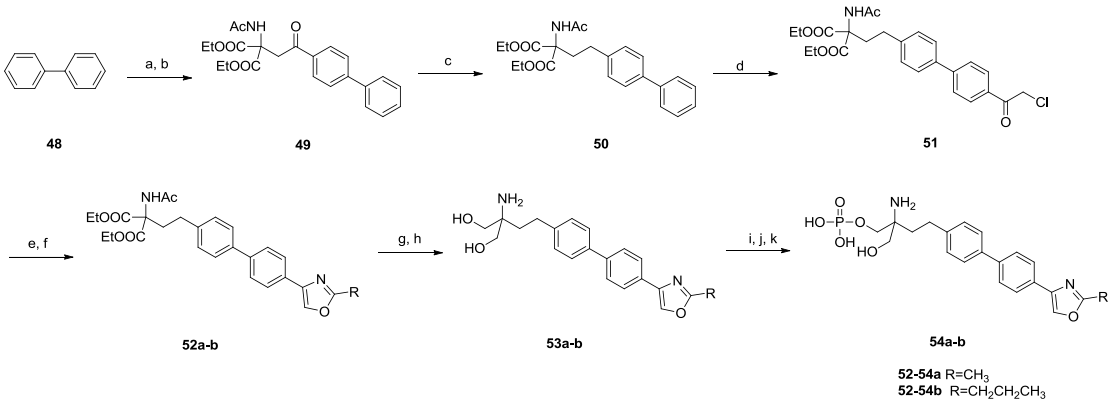

Scheme 4. Reagents and conditions: (a) bromoacetyl bromide, $AlCl_3$, CH_2Cl_2, 0°C to r.t., 2h; (b) diethyl acetamidomalonate, NaH, THF, 70°C, 12h; (c) Et_3SiH, $TiCl_4$, CH_2Cl_2, r.t., 12h; (d)chloroacetylchloride, $AlCl_3$, CH_2Cl_2, 0°C to r.t., 5h; (e) carboxylic acid, Et_3N, CH_3CN, reflux, 2h; (f) acetamide, $BF_3 \cdot Et_2O$, xylene, reflux, 40h; (g) $NaBH_4$, K_2HPO_4 buffer, EtOH, rt, 12h; (h)NaOH, MeOH, 80°C, 8h; (i)CbzCl, $NaHCO_3$, ethyl acetate, rt, 4h; (j)TBPP, Ag_2O, Hex_4NI, CH_2Cl_2, rt, 20h; (k) H_2, Pd/C, MeOH, rt, 8h;

Biological evaluation

$S1P_1$ and $S1P_3$ agonistic activities of these final compounds were evaluated by IP_1 functional assay.[15] As shown in table **1**, biphenyl ether scaffold was considered as a good moiety for $S1P_1/S1P_3$ selectivity enhancement (**14i**, **21a-e**, **25a-c**, **30a-c**, **33**). In general, replacement of biphenyl ether with flexible scaffolds yielded less selectivity (**14a-b, 14d-e**), with the exception of **14c** which showed an unexpected good $S1P_1/S1P_3$ selectivity (9-fold). Compounds with scaffold stronger than biphenyl ether, such as naphthyl, chromone and biphenyl, often have lower potency (**14f-14h**, **54a-b**). These results indicated that proper structure rigidity is preferable for increasing $S1P_1$ potency and selectivity. Introduction of chlorine and fluorine into biphenyl ether scaffold was helpful to improve both the $S1P_1$ potency and $S1P_1/S1P_3$ selectivity (**40a-c**, **47**). **40c** was found to be the most potent $S1P_1$ agonist with a 350-fold $S1P_1$

Published on 03 July 2013. Downloaded on 18/07/2013 09:13:58.

Medicinal Chemistry Communications Accepted Manuscript

View Article Online
DOI: 10.1039/C3MD00079F

selectivity over $S1P_3$.

Table 1 $S1P_1$ and $S1P_3$ agonistic activities of 2-substituted 2-aminopropane-1, 3-diols [a]

compound	$S1P_1$ EC_{50}(nM)	$S1P_3$ EC_{50}(nM)	compound	$S1P_1$ EC_{50}(nM)	$S1P_3$ EC_{50}(nM)
3	14	44	**21e**	254	1711
5	117	>5000	**25a**	51	383
14a	91.5	130	**25b**	529	>5000
14b	37	21	**25c**	329	2197
14c	72	674	**30a**	40.9	1273
14d	203	3.72	**30b**	89	1000
14e	341	184	**30c**	19.8	1130
14f	886	2100	**33**	48.1	113
14g	932	1000	**40a**	66.3	1790
14h	800	508	**40b**	52.9	204
14i	66.3	302	**40c**	14	>5000
21a	85.8	391	**47**	27	349
21b	172	225	**54a**	876	1000
21c	157	1739	**54b**	632	1000
21d	35	1141			

[a]EC_{50} is the mean of three experimental determinations.

Based on these *in vitro* data, compounds **24a** and **39c** (the corresponding alcohol form of compounds **25a** and **40c**) were evaluated *in vivo* for lymphopenia activities, with FTY720 as the control. The number of lymphocytes in peripheral blood was counted 24 h after oral administration of 1 mg/kg of each compound to Sprague Dawley rats. As illustrated in Figure **2**, both **24a** and **39c** showed excellent *in vivo* activity equivalent to FTY720. Meanwhile, the influence on heart rate was also determined in SD rats after oral administration of 10 mg/kg of the compounds. Both **24a** and **39c** showed much less effects on heart rate than FTY720 (Figure **3**).

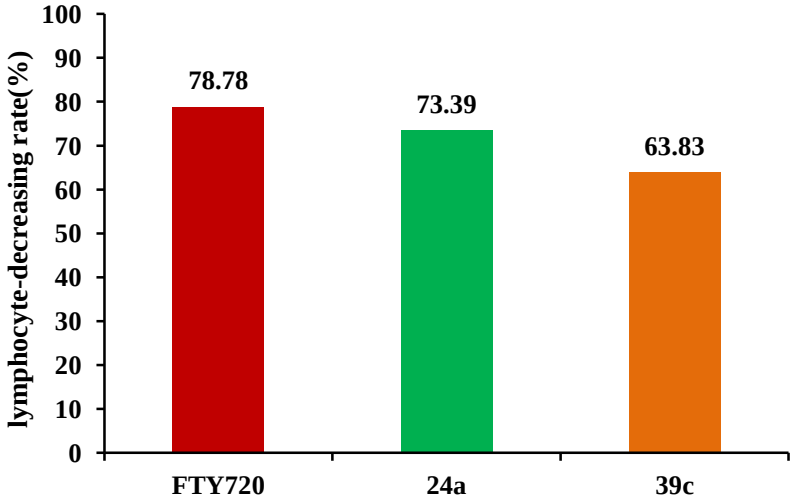

Figure 2 The maximum lymphocyte-decreasing rate within 24h after 1 mg/kg oral administration of **FTY720**, **24a**, **39c** to SD rats.

Published on 03 July 2013. Downloaded on 18/07/2013 09:13:58.

Medicinal Chemistry Communications Accepted Manuscript

View Article Online
DOI: 10.1039/C3MD00079F

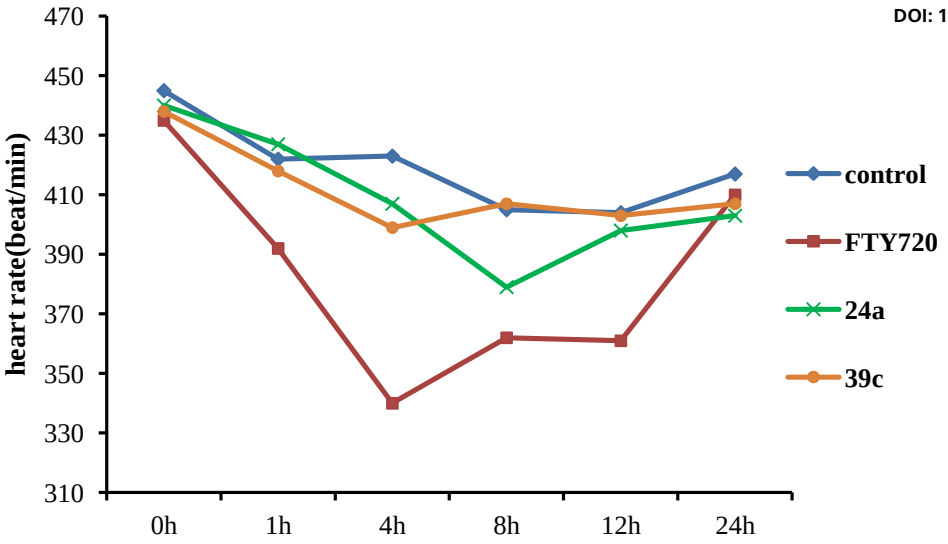

Figure 3 Effect on heart rate in 0, 1, 4, 8, 12 and 24 h after 10 mg/kg oral administration of vehicle and **FTY720**, **24a**, **39c** to SD rats.

Molecular docking

The crystal structure of $S1P_1$ receptor complexing with inhibitor ML056 was obtained from the RCSB protein data bank (PDB entry code: 3V2Y).[10, 16] 29 $S1P_1$ agonists were docked into the active site of $S1P_1$ receptor using Surflex-Dock in SYBYL-X-2.0.[17] All the compounds were grouped into training set and test set containing 21 and 8 compounds, respectively. Both the training and test sets were divided according to a representative range of biological activities and structural variations. The reliability of the docking protocol was checked by comparing the best docking pose obtained for the crystallized inhibitor (ML056) with its bound conformation(Figure **S1**).[18] As a result, a root mean square deviation (RMSD) of 0.897 Å was found suggesting that the docking procedure could be relied on to predict the binding mode of the compounds.

Compound **3**(FTY720-P) was taken as the representative to elucidate the binding mode of agonists to S1P receptor (Figure **4**). It was found that FTY720-P formed salt bridge with residue Tyr29, Lys34, Asn101, Ser105, Arg120 and Glu121. According to the site-mutagenesis results, the salt bridge interaction in the binding site of $S1P_1$ receptor plays an important role in determining the level of agonists' agonism.[10] It is believed that Arg120 (blue) and Glu121 (magenta) are the key residues for ligand binding. The guanidyl of Arg120 and the carboxyl of Glu121 form salt bridge with phosphate group and amino-group of FTY720-P, respectively.[9] Moreover, the aliphatic chain and phenyl ring of FTY720-P accommodate to the hydrophobic cavity of $S1P_1$ receptor showing Van der Waals and π-π stacking interactions with side chains of Tyr98, Met124, Phe125, Leu128, Leu195, Thr207, Phe210, Trp269, Leu272, Phe273, Leu276 and Leu297. These interactions have crucial contribution to ligand binding and selectivity. The docking results were consistent with the site-mutagenesis results, providing a reliable binding mode.

Published on 03 July 2013. Downloaded on 18/07/2013 09:13:58.

Medicinal Chemistry Communications Accepted Manuscript

View Article Online
DOI: 10.1039/C3MD00079F

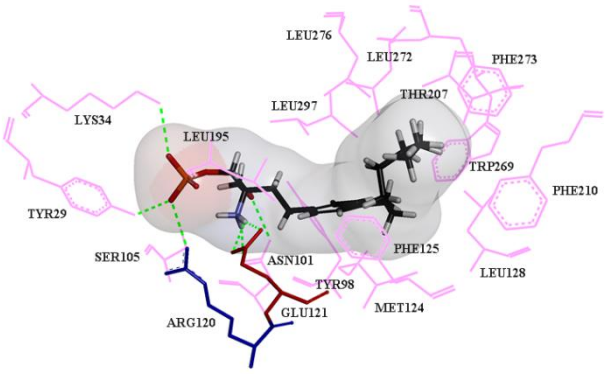

Figure 4 The interactions between **3**(FTY720-P) and the active site of $S1P_1$ receptor. Arg120 is shown in bule and Glu121 is shown in magenta. The green dashed line represents the salt bridge interaction.

3D-QSAR study

To explore the specific contributions of steric, electrostatic, hydrophobic, hydrogen bond acceptor and donor in binding modes for the $S1P_1$ agonists with active site of $S1P_1$ receptor, the alignment of 21 compounds in training set was obtained based on binding conformations in the active site of the receptor (Figure **5**) and used for COMFA and COMSIA model generation.

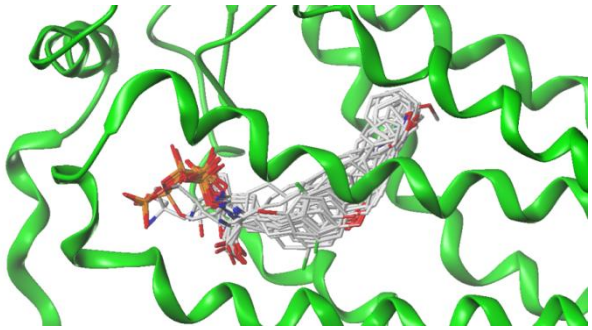

Figure 5 Alignment of agonists in the binding site of $S1P_1$ receptor (shown in green)

COMFA model. The COMFA steric and electrostatic interactions were calculated using SYBYL-X-2.0. PLS analysis[19] results are listed in Table **2**. The value of cross-validated q^2 is 0.547. The noncross-validated PLS analysis with the optimum components of 5 revealed a conventional r^2 value of 0.986, F-value of 215.436 and an estimated standard error of 0.083. The steric field descriptors explain 41.6% of the variance, while the electrostatic descriptors explain 58.4%. The values indicated a good conventional statistical correlation, and the COMFA model had a fair predictive ability. Figure **6**(**A**) shows correlation between actual values and predicted values of 21 compounds and the calculated results are also listed in Table **S1**.

COMSIA model. COMSIA method adds three other descriptors to the COMFA method. These are: hydrogen bond donor, hydrogen bond acceptor and hydrophobic field. The COMSIA results are also summarized in Table **2**. The model showed leave-one-out cross-validation q^2 and conventional r^2 values of 0.544 and 0.943 with the optimum components of 4. The F-value and standard error of estimation are

Published on 03 July 2013. Downloaded on 18/07/2013 09:13:58.

Medicinal Chemistry Communications Accepted Manuscript

View Article Online
DOI: 10.1039/C3MD00079F

65.659 and 0.165, respectively. The steric, electrostatic, hydrophobic, hydrogen-bond donor, and hydrogen-bond acceptor field distributions are 9.8%, 39.9%, 17.5%, 20.6%, 12.2%, respectively. These data indicated that a reliable COMSIA model with satisfactory predictive ability was successfully constructed. Figure **6(B)** shows correlation between actual values and predicted values of 21 compounds and the calculated results are also listed in Table **S1**.

Validation of the 3D-QSAR models. Molecular docking alignment of eight compounds in test set was performed using the same method as that of the training set to validate the QSAR models. The results are simultaneously shown in Figure **6**, Table **S1**. The predicted activities are in good agreement with the observed activities in a statistically tolerable error range, r^2= 0.924 and 0.851 for COMFA and COMSIA model, respectively. These results show that both COMFA and COMSIA model are reliable and can be useful in designing new potent $S1P_1$ agonists.

Table 2 Regression summary of COMFA and COMSIA models

Descriptors	N[a]	q^{2b}	r^{2c}	r^2_{pred}[d]	SEE[e]	F-value[f]	Field contribution in %[g]				
							S	E	H	D	A
COMFA	5	0.547	0.986	0.924	0.083	215.436	41.6	58.4	--	--	--
COMSIA	4	0.544	0.943	0.851	0.165	65.659	9.8	39.9	17.5	20.6	12.2

[a] Optimum number of components obtained from cross-validated PLS analysis and same used in final non-cross-validated analysis.

[b] Cross-validated correlation coefficient.

[c] Non-cross-validated correlation coefficient.

[d] Predictive r^2.

[e] Standard error of estimation

[f] F -test value.

[g] Field contributions: Steric (S) and electrostatic (E) fields from CoMFA. Steric (S), electrostatic (E), hydrophobic (H), hydrogen bond donor (D), and hydrogen bond acceptor (A) from CoMSIA.

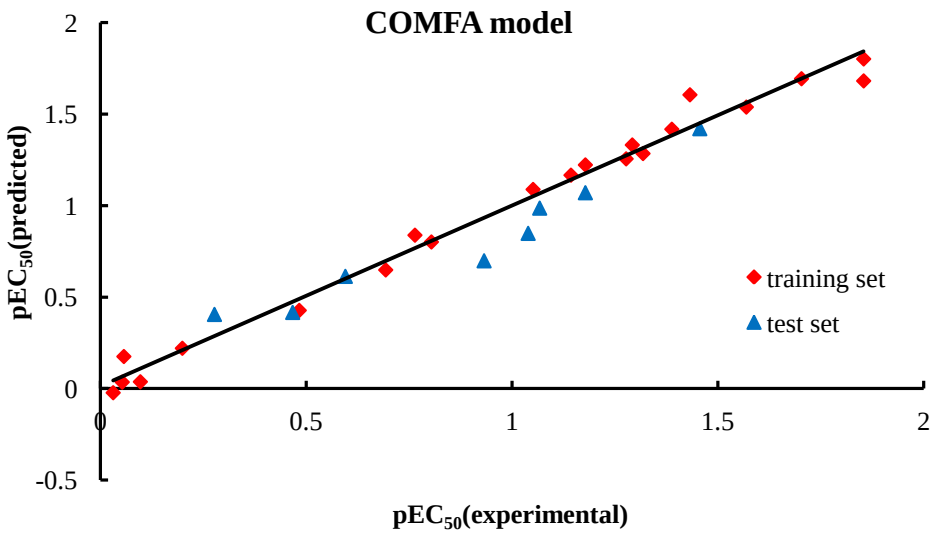

(A)

Published on 03 July 2013. Downloaded on 18/07/2013 09:13:58.

Medicinal Chemistry Communications Accepted Manuscript

View Article Online
DOI: 10.1039/C3MD00079F

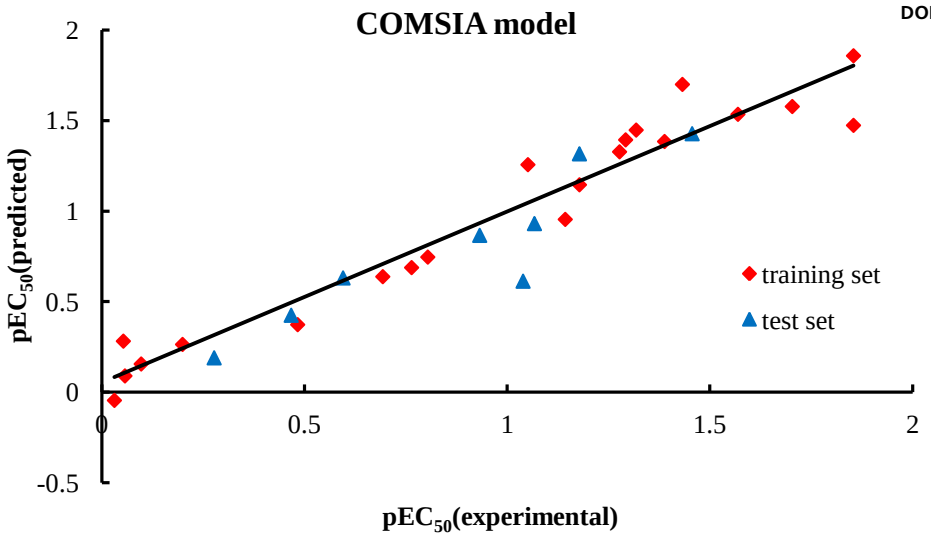

(B)

Figure 6. Correlation between predicted activities by COMFA (A) and COMSIA (B) models and the experimental activities of 29 $S1P_1$ agonists

Interpretation of 3D-QSAR contour maps. Based on COMFA and COMSIA model, the STDEV*COEFF contour maps were constructed. The coefficient contour maps and the binding pocket of $S1P_1$ receptor were superimposed to check whether the variance in the field values corresponding to contours were known to be important for agonist binding and obtain more explicit understanding of the key structural features required for biological activity. To aid in visualization, the most active compound **40c** is displayed in the map (Figure **7**).

The COMFA contour plots of steric and electrostatic interactions are shown in Figure **7a-b**. In the steric fields, green areas indicate regions where bulky groups increase the agonistic activity whereas yellow contours indicate regions where bulky groups decrease the activity (Figure **7a**). Green contours are seen near the phenyl ring close to head group suggesting that bulky substituents in these positions will significantly improve the biological activities. It seems that bulky substituents around this region could form steric interactions with Tyr98, Met124, Leu128, Leu195, Leu272, Trp269 and Leu297. Meanwhile, another green contour is close to the lipophilic tail. That explains why **30c** (R_4=cyclopropyl) is more potent than **30a** (R_4=methyl) and **30b** (R_4=ethyl). Actually, bulky group in this positon would bind to Ile203, Thr207 and Leu276 to favor the activity. There is enough space left to allow bulky group interact with $S1P_1$ receptor residues around the hydrophobic cluster. The yellow polyhedron near the other phenyl ring indicates that bulky substitutions around this position are not favorable. The reason may be that the π-π stacking interactions between agonists and Phe125, Phe273 will be destroyed by bulky group.

In the electrostatic fields, regions where increase positive charge is favorable for agonistic activity are indicated in blue, while regions where increased negative charge is favorable for activity are indicated in red (Figure **7b**). The electrostatic contours are mainly distributed around the head group of **40c**. A large red contour around

Published on 03 July 2013. Downloaded on 18/07/2013 09:13:58.

Medicinal Chemistry Communications Accepted Manuscript

View Article Online
DOI: 10.1039/C3MD00079F

phosphate group indicates that negatively charged substituents in this position should increase the agonistic activity. In fact, the negatively charged substituents can form salt bridge interactions between agonists and Arg120, Tyr29 and Lys34. Another red contour near hydroxyl group reveals that the negative charge of oxygen atom avails agonist activity. The reason may be that the oxygen atom acts as a hydrogen bond acceptor to form a hydrogen bond with Asn101. Near the amino group, there are one large blue polyhedron region indicating that positively charged substituents in this position may increase the activity by strengthening the salt bridge interactions between agonists and Glu121. The results show that the head group of agonists is crucial for $S1P_1$ agonism.

The COMSIA contour plots are shown in Figure **7c-g**. The steric and electrostatic contour maps from the COMSIA analysis are generally in accordance with the field distributions of COMFA maps. Besides the structural features already mentioned in the COMFA electrostatic field analysis, there is a blue polyhedron near Glu294 and Tyr98 (Figure **7d**), suggesting that a positive group in that position may form a salt bridge with those two residues to increase the agonistic activity.

For the hydrophobic maps of COMSIA, yellow and white contours indicate that hydrophobic and hydrophilic groups are favored, respectively (Figure **7e**). The yellow contour covers most regions of the molecule especially the phenyl ring and lipophilic tail, indicating that these structural moieties interact with the side chains of residues at the binding site of $S1P_1$ receptor through hydrophobic interaction. Relevant studies have elucidated that hydrophobic residues play crucial roles in determining the target selectivity[9]. Aromatic rings presented in this region lead to hydrophobic interaction increase, thus **21a-e**, **25a-c** (containing three aromatic rings) exhibit high activities. Meanwhile two small hydrophobic disfavored white regions are embedded in the yellow contours, which explain why **14i**, **21d**, **25a**, **30a-c**, **33**, **40c** and **47** with a biphenyl ether scaffold exhibit high activities.

In the COMSIA hydrogen bond donor field, hydrogen bond donor favored regions are represented by cyan contours and unfavorable regions by purple contours (Figure **7f**), while in the hydrogen acceptor field, hydrogen bond receptor favored regions are represented by magenta contours and unfavorable regions by red contours (Figure **7g**). Both cyan and magenta contours are close to the hydroxyl group of **40c**, indicating that hydrogen bond interactions may exist between hydroxyl group and residues such as Asn101. Removal of hydroxyl group may decrease the activity.

Published on 03 July 2013. Downloaded on 18/07/2013 09:13:58.

Medicinal Chemistry Communications Accepted Manuscript

View Article Online
DOI: 10.1039/C3MD00079F

Published on 03 July 2013. Downloaded on 18/07/2013 09:13:58.

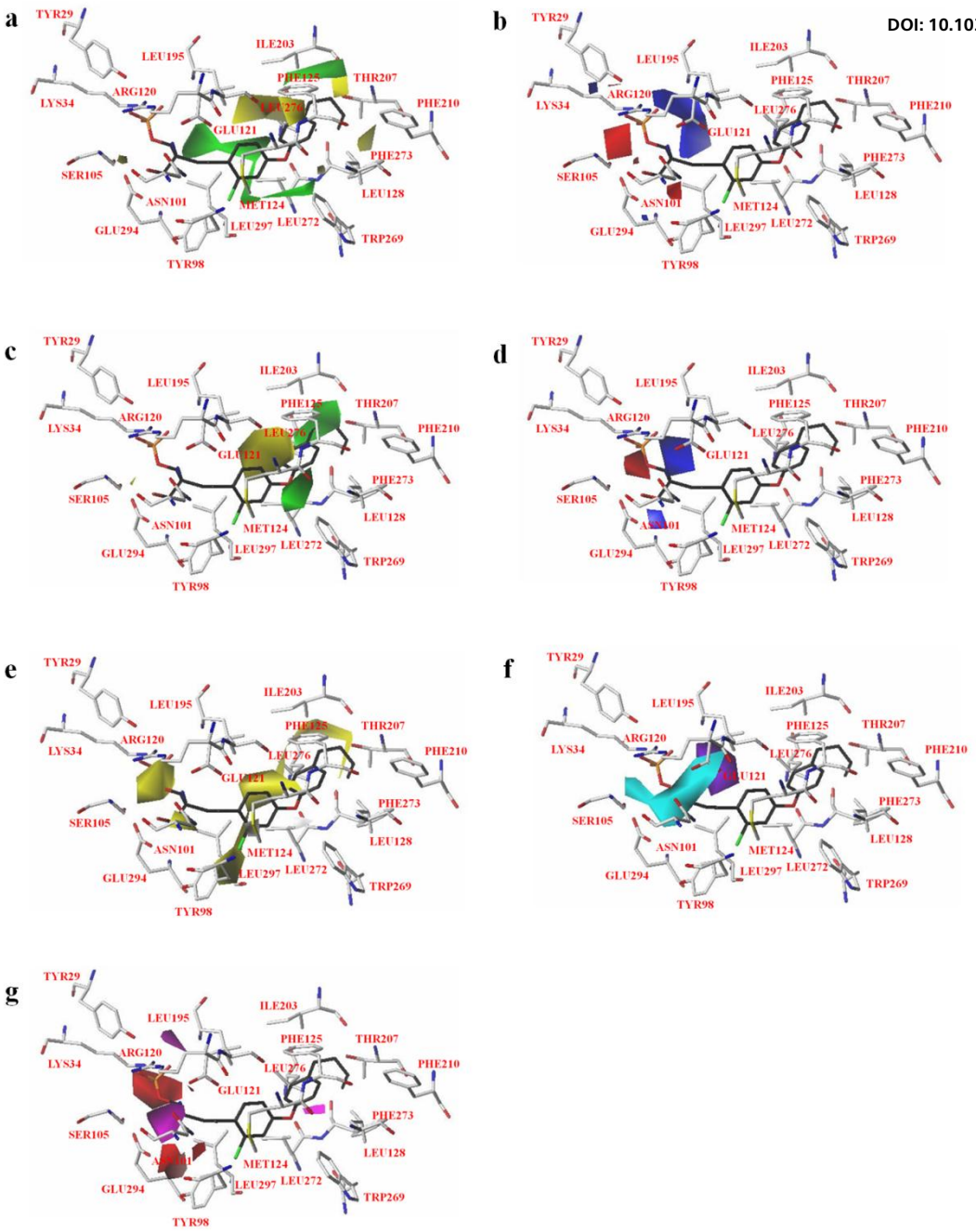

Figure 7. 3D-QSAR contour map displayed with **40c** and superimposition in the active site residues of $S1P_1$ receptor for (a) COMFA steric contour map; (b) COMFA electrostatic contour map; (c) COMSIA steric contour map;(d) COMSIA electrostatic contour map;(e) COMSIA hydrophobic contour map;(f) COMSIA hydrogen bond donor contour map;(g) COMSIA hydrogen bond receptor contour map.

Conclusions

In summary, twenty-seven 2-substituted 2-aminopropane-1,3-diols as $S1P_1$ agonists were designed and synthesized. The initial SARs revealed that properly rigid structures like biphenyl ethers were favorable for these compounds to possess preferable $S1P_1/S1P_3$ selectivity and a chlorine or a fluorine on phenyl rings were also

Medicinal Chemistry Communications Accepted Manuscript

View Article Online
DOI: 10.1039/C3MD00079F

favorable to increase $S1P_1/S1P_3$ selectivity. Compound **40c** showed the most potent $S1P_1$ agonistic activity and the highest $S1P_1/S1P_3$ selectivity. Compound **39c** (alcohol form of compound **40c**) exerted excellent lymphopenia activity and reduced effect on heart rate. High predictive 3D-QSAR modeling towards $S1P_1$ agonists was performed based on molecular docking alignment. Both COMFA (q^2=0.547, r^2=0.986) and COMSIA (q^2=0.544, r^2=0.943) models gave good statistical results in terms of q^2 and r^2 values and matched well with the 3D topology of the binding site of $S1P_1$ receptor. The results provided us significant insights in further understanding of the structure–activity relationship of 2-aminopropane-1,3-diol derivatives and an encouraging way in elucidation of protein–ligand interaction, thereby are useful in the optimization of lead compounds and predicting the activities of new designed agonists.

Published on 03 July 2013. Downloaded on 18/07/2013 09:13:58.

Acknowledgments

This work was financially supported by National Natural Science Foundation of China (NSFC No.81102322 and No.81202545).

Notes and references

1 (a)Y. Sadahira, F. Ruan, S.-i. Hakomori and Y. Igarashi, *Proc. Nati. Acad. Sci.*, 1992, **89**, 9686-9690; (b)H. Rosen, P. J. Gonzalez-Cabrera, M. G. Sanna and S. Brown, *Annu. Rev. Biochem.*, 2009, **78**, 743-768.

2 (a)I. Ishii, N. Fukushima, X. Ye and J. Chun, *Annu. Rev. Biochem.*, 2004, **73**, 321-354; (b)S. E. Gardell, A. E. Dubin and J. Chun, *Trends. Mol. Med.*, 2006, **12**, 65-75.

3 M. Matloubian, C. G. Lo, G. Cinamon, M. J. Lesneski, Y. Xu, V. Brinkmann, M. L. Allende, R. L. Proia and J. G. Cyster, *Nature*, 2004, **427**, 355-360.

4 V. Brinkmann, M. D. Davis, C. E. Heise, R. Albert, S. Cottens, R. Hof, C. Bruns, E. Prieschl, T. Baumruker, P. Hiestand, C. A. Foster, M. Zollinger and K. R. Lynch, *J Biol Chem.*, 2002, **277**, 21453-21457.

5 (a)R. Albert, K. Hinterding, V. Brinkmann, D. Guerini, C. Muller-Hartwieg, H. Knecht, C. Simeon, M. Streiff, T. Wagner, K. Welzenbach, F. Zecri, M. Zollinger, N. Cooke and E. Francotte, *J. Med. Chem.*, 2005, **48**, 5373-5377; (b)A. Billich, F. Bornancin, P. De ́vay, D. Mechtcheriakova, N. Urtz and T. Baumruker, *J Biol Chem.*, 2003, **278**, 47408-47415.

6 S. Mandala, R. Hajdu, J. Bergstrom, E. Quackenbush, J. Xie, J. Milligan, R. Thornton, G.-J. Shei, D. Card, C. Keohane, M. Rosenbach, J. Hale, C. L. Lynch, K. Rupprecht, W. Parsons and H. Rosen, *Science*, 2002, **296**, 346-349.

7 (a)M. G. Sanna, J. Liao, E. Jo, C. Alfonso, M.-Y. Ahn, M. S. Peterson, B. Webb, S. Lefebvre, J. Chun,N. Gray and H. Rosen, *J Biol Chem.*, 2004, **279**, 13839-13848; (b)R. M. Fryer, A. i. Muthukumarana, P. C. Harrison, S. N. Mazurek, Rong, R. Chen, K. E. Harrington, R. M. Dinallo, J. C. Horan, L. Patnaude, L. K. Modis and G. A. Reinhart, PLOS ONE, 2012, 7, e52985.

8 (a)H. Shimizu, M. Takahashi, T. Kaneko, T. Murakami, Y. Hakamata, S. Kudou, T. Kishi, K. Fukuchi, S. Iwanami, K. Kuriyama, T. Yasue, S. Enosawa, K. Matsumoto, I. Takeyoshi, Y.

Medicinal Chemistry Communications Accepted Manuscript

View Article Online
DOI: 10.1039/C3MD00079F

Morishita and E. Kobayashi, *Circulation*, 2005, **111**, 222-229; (b)J. Fujishiro, S. Kudou, S. Iwai, M. Takahashi, Y. Hakamata, M. Kinoshita, S. Iwanami, S. Izawa, T. Yasue, K. Hashizume, T. Murakami and E. Kobayashi, *Transplantation*, 2006, **82**, 804-812.

9 S. C. Schurer, S. J. Brown, P. J. Gonzalez-Cabrera, M.-T. Schaeffer, J. Chapman, E. Jo, P. Chase, T. Spicer, P. Hodder and H. Rosen, *ACS Chem. Biol.*, 2008, **3**, 486-498.

10 M. A. Hanson, C. B. Roth, E. Jo, M. T. Griffith, F. L. Scott, G. Reinhart, H. Desale, B. Clemons, S. M. Cahalan, S. C. Schuerer, M. G. Sanna, G. W. Han, P. Kuhn, H. Rosen and R. C. Stevens, *Science*, 2012, **335**, 851-855.

11 R. D. Cramer, D. E. Patterson and J. D. Bunce, *J. Am. Chem. Soc.*, 1988, **110**, 5959-5967.

12 G. Klebe, U. Abraham and T. Mietzner, *J. Med. Chem.*, 1994, **37**, 4130-4146.

13 P. Durand, P. Peralba, F. Sierra and P. Renaut, *Synthesis*, 2000, **2000**, 505–506.

14 S. Takeda, M. Chino, M. Kiuchi and K. Adachi, *Tetrahedron Lett.*, 2005, **46**, 5169-5172.

15 (a)A. Shenker, P. Goldsmith, C. G. Unson and A. M. Spiegel, *J. Biol. Chem.*, 1991, **266**, 9309-9313; (b)C. Ballatore, J. H. Soper, F. Piscitelli, M. James, L. Huang, O. Atasoylu, D. M. Huryn, J. Q. Trojanowski, V. M. Lee, K. R. Brunden and A. B. Smith, *J. Med. Chem.*, 2011, **54**, 6969-6983.

16 A. L. Parrill, S. Lima and S. Spiegel, *Sci Signal*, 2012, **5**, pe23.

17 A. N. Jain, *J. Med. Chem.*, 2003, **46**, 499-511.

18 C. Tintori, M. Magnani, S. Schenone and M. Botta, *Eur. J. Med. Chem.*, 2009, **44**, 990-1000.

19 B. L. Bush and R. B. Nachbar, Jr., *J. Comput. Aided Mol. Des*., 1993, **7**, 587-619.

Published on 03 July 2013. Downloaded on 18/07/2013 09:13:58.

Medicinal Chemistry Communications Accepted Manuscript